Preprints of the 20th World Congress
The International Federation of Automatic Control
Toulouse, France, July 9-14, 2017

Vision Only Collision Detection with Omnidirectional Multi-Camera System ⋆

Péter Bauer * **Antal Hiba** **

* *Systems and Control Laboratory, Institute for Computer Science and Control (SZTAKI), Hungarian Academy of Sciences (MTA), Budapest, Hungary (Corresponding author e-mail: bauer.peter@sztaki.mta.hu).*
** *Computational Optical Sensing and Processing Laboratory, Institute for Computer Science and Control (SZTAKI), Hungarian Academy of Sciences (MTA), Budapest, Hungary*

Abstract: This article presents an omnidirectional multi-camera system applied to monocular image based visual aircraft sense and avoid. The proposed system can cover 360 degrees horizontal field fo view and so estimate possibility of collision even for intruders coming from backward. First, the definitions of time-to-collision (TTC) and closest point of approach (CPA) are summarized then a simple image parameter based method is proposed for their estimation even in case of oblique camera placement relative to aircraft forward direction. An error analysis of the applied approximation formula is done and a solution to pass past measurements from one camera coordinate system to another if the intruder moves is also presented. Finally a six camera system covering all the horizontal plane is proposed and simulated in software-in-the-loop. A large range of collision and non collision situations with different intruder sizes, velocities, miss distances and flight directions is tested. The validity of decisions is evaluated and the further development directions are determined.

Keywords: Sense and avoid, Computer vision, Multi-camera, Collision decision

1. INTRODUCTION

Sense and avoid (S&A) capability is a crucial ability for the future unmanned aerial vehicles (UAVs). It is vital to integrate civilian and governmental UAVs into the common airspace according to EU (2013) for example. At the highest level of integration Airborne Sense and Avoid (ABSAA) systems are required to guarantee airspace safety.

In this field the most critical question is the case of non-cooperative S&A for which usually complicated multi-sensor systems are developed (see Salazar et al. (2013) for example). However, in case of small UAVs the size, weight and power consumption of the onboard S&A system should be minimal. Monocular vision based solutions can be cost and weight effective therefore especially good for small UAVs see e. g. Degen (2011); Watanabe (2008); Forlenza (2012); Lyu et al. (2016). The author's previous work Bauer et al. (2016) derived a simple and effective method to determine time-to-collision (TTC) and relative closest point of approach (CPA) from intruder camera image size and position. The basics were laid down considering a forward looking camera and error analysis and decision threshold selection methodology were all presented.

However, usually the camera systems consists of more than one camera so the forward looking camera assumption is not always true (see the presented system in e. g. Zsedrovits et al. (2016) with two cameras placed oblique relative to the forward direction). This possibly needs some modification of the formulae. In a multi-camera system passing the past image information from the coordinate frame of one camera to another should be also considered.

Speijker et al. (2012) explicitly requires 360° horizontal field of regard from a sense and avoid camera system so a multi-camera omnidirectional system covering 360° horizontal field of view (FOV) is required. Omnidirectional S&A system developments can be found in e. g. Luis et al. (2011); Finn and Franklin (2011). The former applies a dioptric system (fisheye camera) while the latter applies acoustic sensors. To apply our pinhole camera model based proposed method the lens distortion should be corrected. In case of a fisheye lens this causes larger errors as one approaches the boundary of the lens than with standard lenses . That's why its worth to examine the possibility to create an omnidirectional system from a set of cameras with standard lenses.

The current article considers collision scenarios when the aircraft fly on straight line paths with constant velocity. It targets to examine the required modifications of the formulae presented in Bauer et al. (2016) if the camera is oblique (not parallel withaircraft (A/C) forward axis) and the possibility to pass past image information between the camera frames in a multi-camera system. An error analysis of the proposed approximation formula is also done. Based on these results an omnidirectional multi-camera system is considered which covers the whole horizontal plane and can calculate TTC and CPA value(s) for an intruder coming from any direction. The final outcome of the presented algorithm is the decision about the need to

⋆ This work was supported by the Institute for Computer Science and Control (SZTAKI) Grant Number 008

execute avoidance. First, the definition of TTC and CPA and their estimation with oblique camera are presented in Section 2. The passing of past image data between camera frames is examined in Section 3. Section 4 presents an example omnidirectional system with multiple cameras which can decide about collision for intruders coming from any direction. Software-in-the-loop test results are presented to prove applicability. Finally, section 5 concludes the paper.

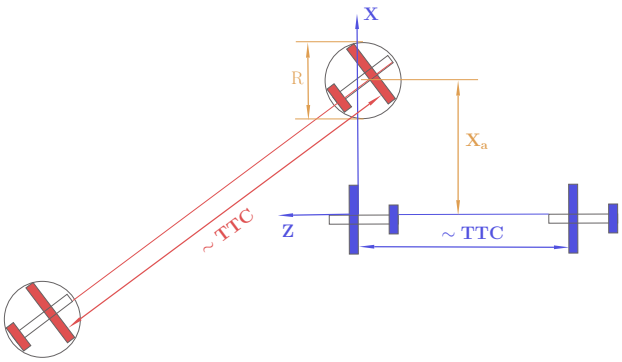

Fig. 1. Define TTC and $CPA = X_a/R$ (intruder red from left, own aircraft blue from right)

2. TTC AND CPA CALCULATION FOR OBLIQUE CAMERA

Firstly, TTC and CPA can be defined considering Fig. 1. Time to collision (TTC) is defined as the flight time until the intruder crosses the X axis of the own aircraft body coordinate system (note that in this work body coordinate systems are defined based-on image processing conventions with forward looking Z and down looking Y axes). This does not necessarily means a collision as the figure shows. The closest point of approach (CPA) is understood relative to the size of the intruder as $CPA = \frac{X_a}{R}$. This is enough for sense and avoid because intruders coming closer than a multiple of their characteristic size can be avoided. Note that if the intruder flies along the body X axis neither TTC nor CPA can be defined.

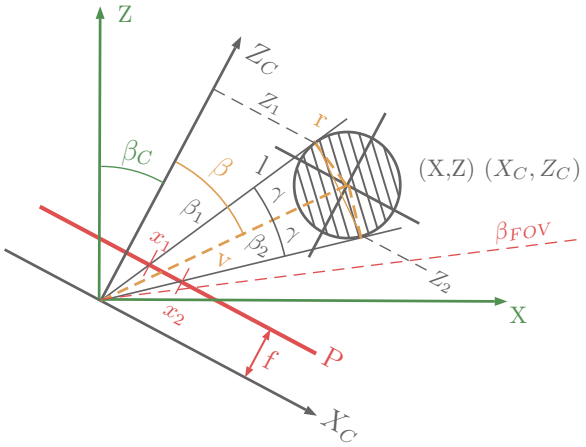

Fig. 2. Oblique camera disc model

An oblique camera setup is shown in Fig. 2 where (X,Z) is the (aircraft) body frame and (X_C, Z_C) is the camera frame rotated by β_C angle relative to the body. The disc represents the intruder aircraft (with half size r (size $R = 2r$)). Note that only the handling of the horizontal intruder coordinates will be discussed throughout the paper. TTC and CPA estimation in the vertical (Y,Z) plane can be done analogously.

For the x position and S size of the intruder image in plane P the following formulae can be derived considering the notations in the figure (for more details see Bauer et al. (2016)).

$$x = f\frac{X_C Z_C}{Z_C^2 - r^2}, \quad S = f\frac{2rl}{Z_C^2 - r^2} \tag{1}$$

Here, X_C, Z_C represent the coordinates of the intruder (disc) object in the camera frame, l is defined later in (2). Considering the Z_1 and Z_2 coordinates in Fig. 2 they can be constructed as $Z_1 = Z_C - \Delta Z_C + \Delta r$ and $Z_2 = Z_C - \Delta Z_C - \Delta r$. ΔZ_C is the projection of the line segment between point (X_C, Z_C) and the intersection point of $\overline{Z_1 Z_2}$ with v to the Z_C axis and Δr is the projection of r to the Z_C axis. This leads to the expression presented in (2). Substituting this into (1) gives an overly complicated expression however, by approximating ΔZ_C as shown in (3) leads to acceptably complicated expressions in (4).

$$\begin{aligned} \cos(\beta_1) + \cos(\beta_2) &= \frac{Z_1}{l} + \frac{Z_2}{l} = \frac{2Z_C - 2\Delta Z_C}{l} \\ l &= \sqrt{X_C^2 + Z_C^2 - r^2} = \frac{2Z_C - 2\Delta Z_C}{\cos\beta_1 + \cos\beta_2} \end{aligned} \tag{2}$$

$$\Delta Z_C = \frac{r^2 Z_C}{X_C^2 + Z_C^2} \approx \frac{r^2}{Z_C} \tag{3}$$

$$\begin{aligned} \bar{S} &= S(\cos\beta_1 + \cos\beta_2) = \frac{2fR}{Z_C} \\ \bar{x} &= x\left(1 - \frac{\bar{S}^2}{16f^2}\right) = f\frac{X_C}{Z_C} \end{aligned} \tag{4}$$

The precision of the approximation in (3) depends on the intruder direction β relative to the camera frame. For $\beta = 0°$ $X_C = 0$ and so there is no approximation. By increasing β (moving the intruder towards the edge of FOV) X_C and so the approximation error will increase. The relative error in ΔZ_C can be derived to be characterized by $\frac{X_C^2}{Z_C^2}$. As β increases this can go as high as 50% at $\beta = 35°$ for example. However, the ΔZ_C approximation is used to approximate l in (2) and so finally the error in l should be characterized.

A very important aspect is that the validity of all formulae is limited by the position of the intruder. If part of it is out of camera FOV then its detection can be questionable. That's why the error caused in l should be examined until the disc - modelling the intruder - is completely in camera FOV. This requires $\beta_2 \leq \beta_{FOV}$ on the positive side (see Fig. 2, β_{FOV} is the angle of the edge of FOV in camera system). From this, intruder position limit values can be derived as summarized below:

$$\gamma_{LIM} = \beta_{FOV} - \beta, \quad l_{LIM} = \frac{r}{\tan\gamma_{LIM}}$$
$$Z_{LIM} = \frac{r\sqrt{1+(\tan\beta_{FOV})^2}}{\tan\beta_{FOV} - \tan\beta} \tag{5}$$

The precision of approximation can now be evaluated by calculating l_{LIM} and Z_{LIM} from (5) and applying (3) and (2) to Z_{LIM} to obtain the approximated l. Fig. 3 shows the percentage errors of l depending on β intruder direction and r intruder half size. $\beta_{FOV} = 35°,\ \beta = 0:30°,\ r = 0.5:30.5m$ were selected as input parameters. The figure shows that the error is below 1 percent in every case which is an excellent result. This shows that the camera will loose the intruder earlier then the error of l increases to unacceptable levels. Fig. 4 shows the Z_{LIM} values below which part of the disc will be out of the camera FOV. The minimum value is about $0.8m$ (for $\beta = 0°,\ r = 0.5m$) while the maximum is about $300m$ (for $\beta = 30°,\ r = 30.5m$).

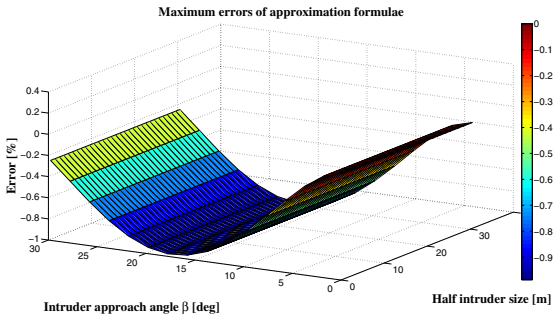

Fig. 3. Errors caused by the approximation of ΔZ_C

Considering now the (X,Z) intruder coordinates in the body frame characterized by the X_a miss distance, the $V_x,\ V_z$ relative velocities and the t_{TC} time to collision (same as TTC) and executing the body to camera frame transformation one gets the $X_C,\ Z_C$ coordinate pair.

$$\begin{aligned} &X = X_a - V_x t_{TC}, \quad Z = -V_Z t_{TC} \\ &X_C = \cos\beta_C X - \sin\beta_C Z \\ &Z_C = \sin\beta_C X + \cos\beta_C Z \\ &X_C = X_a\cos\beta_C - (V_x\cos\beta_C - V_z\sin\beta_C)t_{TC} \\ &Z_C = X_a\sin\beta_C - (V_x\sin\beta_C + V_z\cos\beta_C)t_{TC} \end{aligned} \tag{6}$$

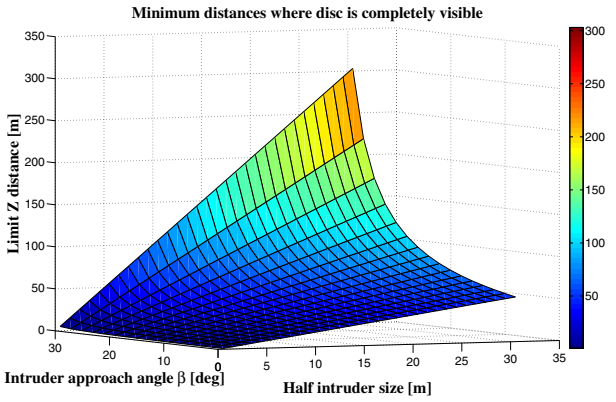

Fig. 4. Minimum Z distances to have disc in camera FOV

Substituting now the expressions of X_C and Z_C into the expressions for $\bar{x}$ and $\bar{S}$ in (4) and considering $CPA = \frac{X_a}{R}$ one gets:

$$\begin{aligned} \frac{1}{\bar{S}} &= \frac{CPA}{2}\frac{\sin\beta_C}{f} - \frac{V_x\sin\beta_C + V_z\cos\beta_C}{2fR}t_{TC} \\ \frac{\bar{x}}{\bar{S}} &= \frac{CPA}{2}\cos\beta_C - \frac{V_x\cos\beta_C - V_z\sin\beta_C}{2R}t_{TC} \end{aligned} \tag{7}$$

In this system of equations the unknowns are CPA and t_{TC} and the time varying terms are $\bar{x},\ \bar{S},\ t_{TC}$. The other terms such as the camera focal length f, the camera angle β_C, the relative velocities $V_x,\ V_z$ and the intruder size R are all constant. Considering this and $t_{TC} = t_C - t$ one gets (t is actual time, t_C is the time of collision):

$$\begin{aligned} \frac{1}{\bar{S}} &= \frac{\sin\beta_C}{f}\frac{CPA}{2} - a_1 t_C + a_1 t = c_1 + a_1 t \\ \frac{\bar{x}}{\bar{S}} &= \cos\beta_C\frac{CPA}{2} - a_2 t_C + a_2 t = c_2 + a_2 t \end{aligned} \tag{8}$$

Fitting least squares (LS) optimal linear curves to the expressions gives a_1, a_2, c_1, c_2. These fits require at least two data points but possibly 8-10 points should be used to suppress the effect of pixelization and other image noises. From the estimated coefficients a system of linear equations results for $CPA/2$ and t_C:

$$\begin{bmatrix} \frac{\sin\beta_C}{f} & -a_1 \\ \cos\beta_C & -a_2 \end{bmatrix} \begin{bmatrix} \frac{CPA}{2} \\ t_C \end{bmatrix} = \begin{bmatrix} c_1 \\ c_2 \end{bmatrix} \tag{9}$$

The system of equations is solvable if the coefficient matrix on the left hand side is invertible. Consdiering its determinant and the expressions for a_1 and a_2 one gets (10). The expression is not zero until $V_z \neq 0$ this means that the intruder angle relative to the body frame $\beta_a = \beta_C + \beta$ satisfies $-90° < \beta_a < 90°$. This is the same range in which the definitions of CPA and TTC are valid. Possibly, the problem is also solvable if the intruder approaches the body system from behind with $V_z < 0$ but this will be the topic of future research.

$$\begin{aligned} &\begin{vmatrix} \frac{\sin\beta_C}{f} & -a_1 \\ \cos\beta_C & -a_2 \end{vmatrix} = -a_2\frac{\sin\beta_C}{f} + a_1\cos\beta_C = \\ &= -\frac{V_x\cos\beta_C - V_z\sin\beta_C}{2R}\frac{\sin\beta_C}{f} + \\ &+ \frac{V_x\sin\beta_C + V_z\cos\beta_C}{2fR}\cos\beta_C = \frac{V_z}{2fR} \neq 0 \end{aligned} \tag{10}$$

3. PASSING PAST IMAGE DATA BETWEEN CAMERA FRAMES

In a multi-camera system cameras should be placed so that their FOVs overlap each other. The image of the intruder will usually move from one camera FOV to another during an approach. Considering that the LS fit to estimate TTC and CPA uses multiple (8-10) points this will cause a problem if we have the previous 7-9 points in the previous camera frame and the new one in the new. Transformation

of the past information (points) to the new frame should be solved.

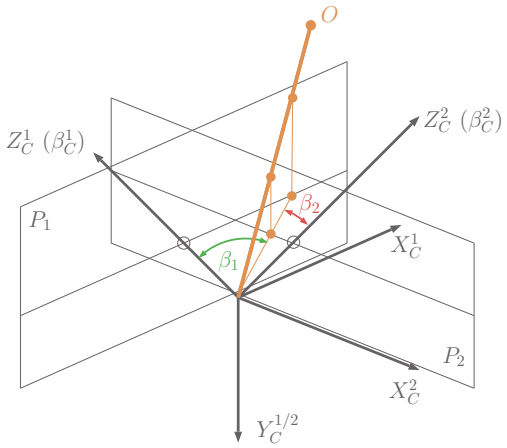

Fig. 5. Representation of the horizontal component of a vector in two camera frames

The LS line fit is based on the $\bar{x}$ and $\bar{S}$ values which are obtained by transforming x and S (intruder image centroid and intruder image size) measured values see (4). So $\bar{x}$ and $\bar{S}$ can not be considered for transformation between the camera frames. The method of image processing first estimates intruder image centroid (x) and 'corner point' ($x_{c_1} - x_{c_4}$) positions, then makes an ego motion compensation relative to the flight trajectory (see Degen (2011)). The transformed centroid position is considered as x in (1) and the S intruder size is derived from the minimum and maximum of transformed $x_{c_1} - x_{c_4}$ points. So it is straightforward to store the x and $x_{c_1} - x_{c_4}$ values after ego motion compensation in a form common between the different camera frames. The representation of one point (O object) is visualized in Fig. 5. It is assumed that the camera frame origins are in one point. In a real system their distances can be a few centimeters so the assumption is approximately true compared to the few tens to hundreds meters distance of an intruder.

Considering the figure the common information about O in the horizontal plane is the angle of the horizontal projection of the frame origin - O vector relative to the two frames (β_1 and β_2). If originally camera 1 (frame 1) tracks the object, the time stamped β_1 values are saved. If the object moves to the other camera (frame 2) its position can be represented by β_2. Considering the camera setting angles (β_C^1 and β_C^2) the transformation of measured β_1 values to β_2 is straightforward:

$$\beta_2 = \beta_1 + \beta_C^1 - \beta_C^2$$

In case of camera change it is easy to execute this transformation for the stored centroid and corner point β angles and then obtain x, S and so $\bar{x}$ and $\bar{S}$ in the new frame. This makes it possible to continue LS line fit with minimum errors in case if the intruder moves from one camera FOV to another. Note that in case of the vertical (Y) coordinates there is no need for transformation if the $X - Z$ planes of all camera frames are in the same horizontal plane. This is a realistic assumption regarding most of the multi-camera systems.

4. EXAMPLE OMNIDIRECTIONAL CAMERA SYSTEM AND TEST RESULTS

After formulating all the theoretical basics it is possible to construct an example omnidirectional system covering 360° FOV and test it in software-in-the-loop (SIL) simulations. The example six camera system (each camera with 70° FOV which means a 10° overlap between them) is shown in Fig. 6 together with camera angles relative to the front body frame. As shown with (10) one body frame is not enough to define TTC and CPA for any intruder direction. That's why in this example four body coordinate systems are defined as shown in Fig. 7.

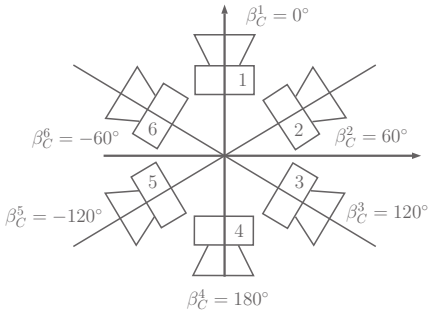

Fig. 6. Example six camera system

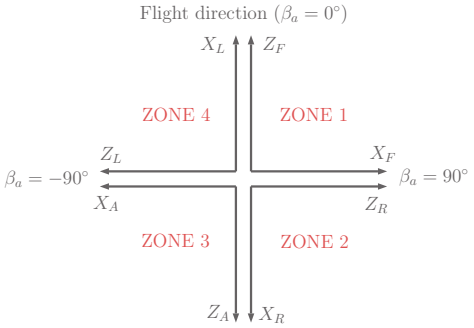

Fig. 7. Multiple body coordinate systems

Four body systems can cover the whole 360° range. This case there is always a system facing the intruder. Possibly a lower number of systems can be also satisfactory, but this will be the topic of future research. Of course, in the calculation of TTC and CPA the β_C angle of the camera frame should be given relative to the actual body frame. The notations are as follows: F front, R right, A aft and L left systems. Four zones are defined considering possible intruder directions relative to the front body system based-on the β_a relative angle. In every zone the TTC and CPA values can be calculated in two body frames parallelly and the collision decision done considering the values which first become critical. The summary of zones:

- ZONE 1: $0° \leq \beta_a < 90°$, *front* and *right* systems
- ZONE 2: $90° \leq \beta_a < 180°$, *right* and *aft* systems
- ZONE 3: $-180° \leq \beta_a < -90°$, *aft* and *left* systems
- ZONE 4: $-90° \leq \beta_a < 0°$, *left* and *front* systems

The TTC and CPA estimation is implemented in a Matlab Simulink SIL simulation applying the dynamic model of two aircraft together with autopilot control loops. Based on the aircraft positions the projection of a simplified 3D geometrical representation of the intruder to the camera image planes is done with 8fps (for details see Bauer et al. (2015)). Pixelization errors are introduced and the visibility of the intruder is considered. It is not visible by the camera if its behind it, its smaller size is below one pixel or part of it is out of camera FOV. In this setup maximum two camera observe the intruder at the same time. The change between camera frames is done when the intruder is again in the FOV of only one camera. In the overlap region tracking and calculations are done in the camera frame which first observed the intruder. LS optimal line fits are done for 8 data points.

A large set of possible intruder sizes and velocities is considered as described in detail in Bauer et al. (2015) (see Table 1). The own A/C velocity is fixed to 20 m/s. The aircraft straight tracks are designed to have fixed intruder angle relative to the front body system of own aircraft if $CPA = 0$ see the right side of Fig. 8.

Table 1. Intruder sizes and velocities

Wingspan [m]	3.5	10	20	40	60
V_{min} [m/s]	10	39	52	133	205
V_{mean} [m/s]	25	72	145	222	241
V_{max} [m/s]	40	147	256	265	257
Success rate [%]	97	98	94	100	100

In the figure V_o and V_i are the own and intruder velocity vectors respectively, β_a is the intruder view angle (intruder angle relative to front body frame) and β_3 is the required angle of the intruder track relative to own aircraft track. The goal is to have constant β_a and so constant view angle of the intruder from the camera while the aircraft are flying along their track. This requires that the line L should not rotate which is equivalent to $V_i \sin\beta_2 = V_o \sin\beta_a$ From this β_2 can be calculated and so $\beta_3 = \beta_a + \beta_2$ can be obtained. This guarantees that for zero CPA the view angle will be the given value. For nonzero CPA values this is not true but tests were also run. Nonzero CPA is represented by the left part of the figure with X_a miss distance between the aircraft. The altitude of the aircraft is set to be the same and constant.

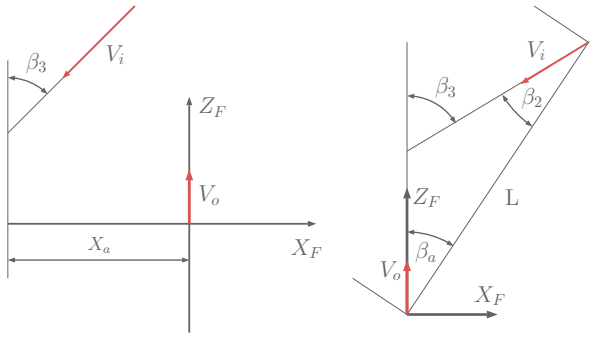

Fig. 8. Track design for own aircraft and intruder (nonzero CPA left, zero CPA right)

The β_a angle was set as [0, 30, 60, 90, ... 270, 300, 330] degrees (relative to the front body frame) in order to create critical situations with zero CPA when the intruder comes on the boundary of two camera FOVs (in the middle of the overlapping region). These values are [30, 90, 150, 210, 270, 330] degrees and its really important to test the methods in such critical situations as will be shown later. The considered CPA values were [0, 10, 20]. The TTC decision threshold was set to 2 seconds (if estimated TTC decreases below 2 seconds the collision decision should be done) while the CPA threshold for 15 (to guarantee collision decision for CPA=10 and below considering the uncertainty in CPA estimation in Fig. 10). After deciding about non collision in one body frame this decision can be overwritten if collision situation appears later in the other frame.

The simulation test campaign (we can call it Monte Carlo simulation) was run for all intruder sizes and velocites - except for the 10m/s velocity at 3.5m size because this is smaller than own velocity so an aft approach is not possible. The X_a miss distances were calculated from CPA and intruder size in every case.

The decision about collision or non collision was correct in all cases when it could be done. In some cases the intruder was continuously in the overlapping region of two cameras but neither of the camera FOVs included the complete aircraft. That's why neither of them could track it and so there was not possible to make a decision. These are the critical situations mentioned before. This problem can be overcome by increasing the overlapping of the cameras. Otherwise the overall success rates are all well above 90% so this is an acceptable result (see Table 1). Success rate means that in how many percent of the cases was there a successful decision about collision / non collision.

From the test campaign the most interesting result is the comparison of real TTC at the time of decision with the 2 seconds threshold and the comparison of the ratio of estimated CPA and the real one. These are presented in Fig.s 9 and 10.

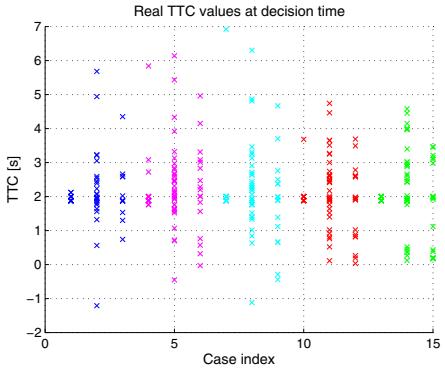

Fig. 9. Real TTC values upon decision

In the figures the case indices indicate the CPA 0, 10, 20 results (the same color) for the different intruder sizes (5 sizes with 3 different CPA value means case indices from 1 to 15). The TTC figure shows that real TTC is around 2 seconds and above in a lot of cases when the estimated TTC decreases below 2 seconds. Staistically 218 cases from 367 are above 2 seconds (48.5%), 149 (40.6%) are above 1 seconds and only 40 (10.9%) are below 1 second. The

cases below 1 second can be critical because then there is not enough time to execute avoidance. The cases between 1 and 2 seconds can be acceptable (it depends on the maneuverability of the own aircraft) and the cases above 2 seconds are perfect.

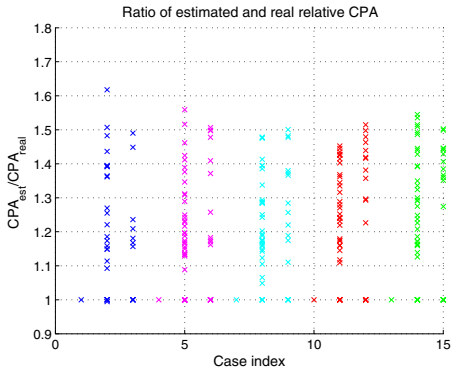

Fig. 10. Ratio of estimated and real CPA

The CPA figure shows that estimated CPA is usually 1.1 - 1.5 times larger than the real CPA. That's why the CPA threshold was selected to be 15 to avoid every intruder arriving below CPA=10. According to the data the collision / non collision decisions when executed were 100% correct with this threshold. The ratio 1 values in the figure symbolize the cases when both estimated and real CPAs are around 0 that's why their ratio is very uncertain and can distort statistics.

5. CONCLUSION

This paper dealt with monocular image based visual sense and avoid possibilities considering multi-camera systems. After the introduction of the topic it defined time to collision (TTC) and relative closest point of approach (CPA). Then it considered cameras placed oblique relative to the own aircraft forward axis and derived a simple image parameter based method to estimate TTC and CPA. The developed method is based on least squares optimal line fit to 8-10 data points to smooth effects of pixelization and noise.

In the next part passing of past image data from one image frame to another was considered if the intruder changes from one camera field of view (FOV) to another. This opened up the possibility to create a multi-camera system covering the whole horiztonal range (360 degrees) with its FOV. However, for such a system multiple body coordinate frames should be introduced because otherwise TTC and CPA can not be defined for any intruder direction.

The last part proposed a six camera system which covers the whole horizontal range. TTC and CPA estimation was tested extensively applying Monte Carlo software-in-the-loop simulations. TTC and CPA estimate based decision about the collision was possible in more than 94% of the tested cases. In the other cases the intruder was undetectable because its image was divided between the two cameras. TTC estimation was acceptable in about 89% of the cases. CPA estimates were 1.1 - 1.5 times larger then the real CPA values.

Future work should include examination of the minimum number of required body coordinate systems and increase of CPA estimation precision if possible. Other topics are the consideration of camera misalingment and orientation estimation (in ego motion compensation) errors.

ACKNOWLEDGEMENTS

The authors gratefully acknowledge the contribution of the reviewers to the improvements of the paper.

REFERENCES

Bauer, P., Hiba, A., Vanek, B., Zarandy, A., and Bokor, J. (2016). Monocular Image-based Time to Collision and Closest Point of Approach Estimation. In *In proceedings of 24th Mediterranean Conference on Control and Automation (MED'16)*. Athens, Greece.

Bauer, P., Vanek, B., Peni, T., Futaki, A., Pencz, B., Zarandy, A., and Bokor, J. (2015). Monocular image parameter-based aircraft sense and avoid. In *In proceedings of 23rd Mediterranean Conference on Control and Automation (MED'15)*. Torremolinos, Spain.

Degen, S. (2011). *Reactive Image-based Collision Avoidance System for Unmanned Aircraft Systems*. Master's thesis, Australian Research Centre for Aerospace Automation.

EU (2013). Roadmap for the integration of civil Remotely-Piloted Aircraft Systems into the European Aviation System. Technical report, European RPAS Steering Group.

Finn, A. and Franklin, S. (2011). Acoustic Sense & Avoid for UAVs. In *In Proc. of Seventh International Conference on Intelligent Sensors, Sensor Networks and Information Processing (ISSNIP)*.

Forlenza, L. (2012). *Vision based strategies for implementing Sense and Avoid capabilities onboard Unmanned Aerial Systems*. Ph.D. thesis, UNIVERSITÁ DEGLI STUDI DI NAPOLI FEDERICO II.

Luis, M., Ivan, M., and Pascual, C. (2011). Omnidirectional bearing-only see-and-avoid for small aerial robots. In *In Proc. of the 5th International Conference on Automation, Robotics and Applications*.

Lyu, Y., Pan, Q., Zhao, C., Zhang, Y., and Hu, J. (2016). Vision-Based UAV Collision Avoidance with 2D Dynamic Safety Envelope. *IEEE A&E SYSTEMS MAGAZINE*, 31, 16–26.

Salazar, L.R., Sabatini, R., Ramasamy, S., and Gardi, A. (2013). A Novel System for Non-Cooperative UAV Sense-And-Avoid. In *In Proceedings of European Navigation Conference 2013 (ENC 2013)*.

Speijker, L., Verstraeten, J., Kranenburg, C., and van der Geest, P. (2012). Scoping Improvements to 'See And Avoid' for General Aviation (SISA). Technical report, European Aviation Safety Agency (EASA).

Watanabe, Y. (2008). *Stochastically Optimized Monocular Vision-based Navigation and Guidance*. Ph.D. thesis, Georgia Institute of Technology.

Zsedrovits, T., Bauer, P., Pencz, B.J.M., Hiba, A., Gőzse, I., Kisantal, M., Németh, M., Nagy, Z., Vanek, B., Zarándy, A., and Bokor, J. (2016). Onboard Visual Sense and Avoid System for Small Aircraft. *IEEE A&E SYSTEMS MAGAZINE*, 31, 18–27.